Coke formation on an industrial reforming Pt–Sn/γ-Al$_2$O$_3$ catalyst

C.L. Li [a,*], O. Novaro [a,**], X. Bokhimi [a], E. Muñoz [a], J.L. Boldú [a], J.A. Wang [b], T. López [c], R. Gómez [c] and N. Batina [c]

[a] *Institute of Physics, The National University of Mexico (UNAM), A.P. 20-364, 01000 México D.F., Mexico*
E-mail: novaro@fenix.ifisicacu.unam.mx
[b] *Laboratory of Catalysis and Materials, Superior School of Chemical Engineering (ESIQIE), National Polytechnic Institute of Mexico (IPN),*
Zacatenco, UPALM, 07738 Mexico City, Mexico
[c] *Department of Chemistry, Universidad Autónoma Metropolitana-I, A.P. 55-534, 09340 México D.F., Mexico*

The characterization of the coke deposited on an industrial Pt–Sn/γ-Al$_2$O$_3$ catalyst, used in a continuous reforming process, was performed with AFM, XRD, FTIR, EPR, NMR, TG-DTG and DTA techniques. Composition, structure and location of the coke on the catalyst were investigated. The coke was predominantly deposited on the catalyst surface and in the interstices between the catalyst particles. Its content increased along the reactor from top to bottom. Coke was deposited in the form of uniform films and clusters of three-dimensional disks with diameters between 0.12 and 0.18 μm. It had a pseudo-graphite structure produced by the dehydrogenation and polymerization of the aromatic precursor compounds. The coked catalyst showed a good combustion behavior; it was regenerated below 550 °C. These results are important to elucidate the coke formation mechanism, to generate new continuous reforming catalysts, and to optimize the reactor operation parameters.

Keywords: coke formation, industrial reforming catalyst, Pt–Sn/γ-Al$_2$O$_3$, coke characterization, coke burning off

1. Introduction

Catalytic reforming is one of the most efficient technologies for the production of high-octane gasoline, and for supplying aromatic compounds for BTX units [1]. From them the bimetallic reforming catalysts have been one of the major technical developments in heterogeneous catalysis [2].

In the last decade, the new reforming units have been developed in two different ways: those where the catalyst is regenerated on a one-year on-stream cycle (semi-regenerative), and the one operating with continuous catalyst regeneration (CCR). In a semi-regenerative unit, the catalyst is placed in a fixed-bed reactor, where Pt–Re/γ-Al$_2$O$_3$ or Pt–Ir/γ-Al$_2$O$_3$ catalysts are predominantly used. The extra stability produced by rhenium (iridium) allows performing long cycles [3–5]. In CCR units, the catalyst flows down along the reactor by the action of gravity and is regenerated in a continuous process. In this case, the coke on the catalyst has a constant profile and, therefore, the catalyst activity is close to its initial value. At low-pressure operations, the CCR reforming process also produces high yields of aromatic compounds and hydrogen [6]. This process has also renewed the importance of the Pt–Sn/γ-Al$_2$O$_3$ catalyst, in which, under severe conditions, tin is able to modify the catalyst selectivity for aromatics [7].

Improvement of catalysts for the petrochemical industry is always an actual topic [8–11], because these catalysts are inevitably deactivated by the coke formed via the hydrocarbons used in the catalyzed process. Catalyst activity, however, is usually reversible, since it can be recovered by controlling coke burning off [12,13]. The research about deposited coke on reforming catalysts involves not only its content and location but also its structure and nature. This information will be useful for developing the new-generation catalysts.

All reforming catalysts are now regenerated by combustion under controlled conditions; therefore, it is very important to study the coke burn-off behaviors. There are only a few investigations concerning this topic; for them it is worth to mention those about the coke deposited on Pt–Ir and Pt–Re reforming catalysts in a fixed-bed reactor [14–16]. Very recently, some scientific studies focused on coke formation on the reforming catalyst system have been reported [17,18]. In the reforming units with continuous regeneration where the Pt–Sn/γ-Al$_2$O$_3$ catalyst is used, the severe working conditions produce coke rapidly, requiring frequent regeneration. To ensure high catalytic performance, the Pt–Sn catalyst pellets in the reactor only work for five days, then they are moved into the regenerator for burning the coke off. Coking behavior in CCR units is markedly different from the one observed in semi-regenerative fixed-bed units where the catalyst pellets keep contact with the feed stream for about one year before they are regenerated.

In the present paper, coked and regenerated Pt–Sn/γ-Al$_2$O$_3$ catalysts were taken from an industrial reforming unit with continuous regeneration. Amount and location of the formed coke as well as its nature and composition were characterized. Furthermore, the correlation between coke deposition and combustion was analyzed. The results

provide alternatives not only to develop new reforming catalysts but also to optimize the reactor operation parameters.

2. Experimental

2.1. Sample preparation

Catalyst specimens were discharged from the respective position of an industrial continuous reforming unit. They had an average coke content of 4.2 wt%, measured via the method reported by Li and Gonzalez [19]. This coke concentration was decreased to only 0.04 wt% when the catalyst was regenerated.

Coke was liberated from the catalyst by dissolving the catalyst in a 40% hydrofluoric acid solution. It was obtained by separating the precipitate which was further washed with deionized water and then dried. This treatment does not produce any transformation of the coke and, therefore, the information concerning the composition is reliable [20].

2.2. Catalyst characterization

2.2.1. Analysis of the elements
Carbon to hydrogen ratio of the isolated coke was measured with a MOD 1106 Carlo Erba elemental analyzer. The ratio for the coke on the coked Pt–Sn/γ-Al$_2$O$_3$ catalyst discharged from the bottom of the last reactor was C : H = 1 : 0.51.

2.2.2. Fourier transform infrared spectroscopy (FTIR)
FTIR spectroscopic characterization of the coked catalyst and the isolated coke were performed with a Nicolet Magna-IR550 spectrometer. Spectra were recorded at room temperature.

2.2.3. ^{13}C NMR analysis
^{13}C NMR spectra were obtained with a Bruker ASX 300 spectrometer using the magic angle spinning technique.

2.2.4. X-ray diffraction analysis (XRD)
X-ray diffraction patterns were measured at room temperature with a Siemens D-5000 diffractometer that had Cu Kα radiation. Specimens were prepared by packing sample powder into a glass holder. Intensity was measured by step scanning in the 2θ range between 20° and 110° with a step of 0.02° and a measuring time of 2.7 s per point.

2.2.5. Electron spin resonance (EPR)
Electron spin resonance experiments were carried out on a Jeol JESRE3X spectrometer, using a cylindrical cavity (TE011 mode) operating at X-band frequencies (near 9.15 GHz), with 100 kHz field modulation. The g values were obtained by measuring the resonance field with a NMR gaussmeter ES-FC5 (Jeol) and a frequency counter HP-5350B. Spectra were recorded at different temperatures by using the Jeol DVT2 variable temperature control unit.

MgO : Mn^{2+} was used as the standard field marker, and a NaCl : Mn^{2+} single crystal, in which the manganese content was obtained by atomic absorption spectroscopy, was used as the concentration standard. The EPR quartz tubes containing the sample were evacuated up to 10^{-4} Torr.

2.2.6. Atomic force microscopy (AFM)
Atomic force measurements were performed with a nanoscope IIIa MultiMode scanning probe microscope (Digital Instruments, Inc., Santa Barbara, CA, USA), with a phase extender module. Imaging was performed *ex situ*, under laboratory atmosphere conditions, with the AFM operating in the so-called phase imaging of the tapping mode (DI manual for Nanoscope III-SPM). Commercial Si cantilevers (nanosensors) (TESP, from DI) with spring constants of 31–50 N/m and resonance frequencies of 270–310 kHz were used. In order to avoid sample or tip damaging, images were collected at the scan rate of 1 Hz. Using an optical stereo-microscope, we chose for each sample up to five different places for AFM imaging. In this way, the statistical nature of our analysis was fulfilled. All phase images are presented in a "top-view" mode.

2.2.7. Thermoanalysis
Thermogravimetric (TG) and differential thermal analyses (DTA) were carried out with a Dupont 2000 apparatus. For the TG experiments, about 16 mg of the coked or regenerated catalyst were placed in a pan that was heated in streaming air (120 ml/min) from 25 to 1000 °C at a heating rate of 10 °C/min. For the DTA test done under the conditions mentioned above, 2 mg of the catalyst were placed in the sample pan, and the same amount of the regenerated catalyst was located in the reference pan.

2.2.8. BET specific surface areas and pore distribution
Adsorption isotherms were measured with an automatic sorptometer on a Micromeritics ASAP 2000 apparatus. Samples were reactivated at 300 °C in vacuum (10^{-5} Torr) for 3 h. Specific surface areas and pore size distributions were calculated from the adsorption isotherms using nitrogen as the adsorbent.

3. Results and discussion

3.1. Coke structure and nature

Studies about coke formation have been extensively carried out by using FTIR spectroscopy [21]. There, the band at 1585 cm^{-1} is assigned to the C=C stretching vibration of microcrystalline graphitic carbon structures, which are present in polycyclic aromatic compounds and coke deposits on a Pt/Y-zeolite catalyst. The absorption bands between 900–700 cm^{-1} are assigned to CH-wagging modes of polycyclic aromatics and those between 3060 and 2860 cm^{-1} are assigned to aromatic and aliphatic rings [22].
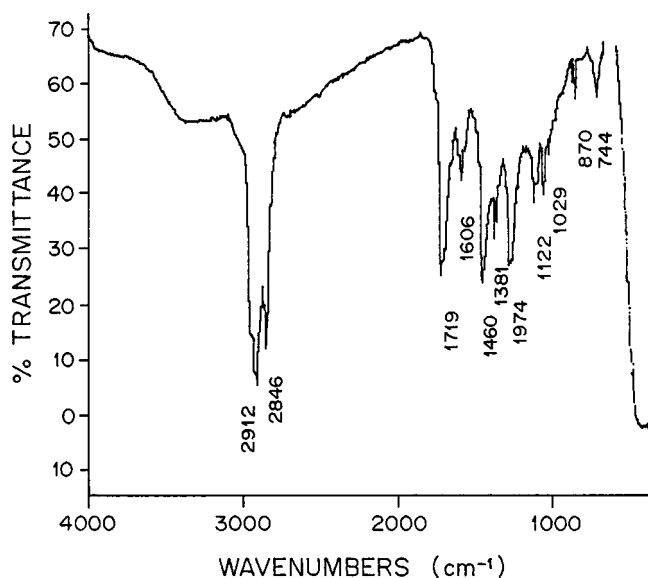
Figure 1. FTIR spectrum of dissolved coke from the coked Pt–Sn/γ-Al$_2$O$_3$ catalyst.

Figure 2. A typical ^{13}C MAS NMR spectrum of the coked Pt–Sn/γ-Al$_2$O$_3$ catalyst.

In the present work, coke was isolated by dissolving the catalyst in hydrofluoric acid because it does not modify the coke. The separation, however, was not complete: small amounts of platinum and alumina were detected by XRD. To avoid misleading conclusions, the coke was at first separated from the coked catalyst by the hydrofluoric acid treatment and then it was extracted with methylchloride in a Soxlet flask. The soluble composition of the coke was taken as a sample for FTIR studies to elucidate the coke formation mechanism.

A typical FTIR spectrum is shown in figure 1. Two absorption bands at 744 and 871 cm^{-1} together with two other little bands in the range of 700–900 cm^{-1} were observed. As mentioned above, they were produced by polycyclic aromatics like pyrene or chrysene. The spectrum has two sharp bands at 2846 and 2912 cm^{-1}, produced by the symmetric and asymmetric flexion vibration of the C–H bonds associated to the CH$_2$ groups connected to the aromatic rings or aliphatic groups. In addition, the band of olefinic flexion vibration was observed at 1606 cm^{-1}, and that for C–H twisting and wagging vibration bands appeared at 1381, 1374 and 1460 cm^{-1}, respectively [23].

Coke nature and structure was also analyzed with ^{13}C NMR [24]. Its spectrum consisted of only one large absorption peak at 125 ppm (figure 2). It is reported that carbon atoms with a sp^2 hybridized state have a chemical shift between 82 and 160 ppm, and those with a sp^3 hybridized state between 0 and 82 ppm. The NMR spectrum shows that the coke deposited on the Pt–Sn/γ-Al$_2$O$_3$ catalysts contained components having polynuclear aromatic and graphite like structures with a sp^2 hybridized state and negligible amounts of –CH$_3$ side chains with a sp^3 hybridized state.

EPR has long been applied in catalysis to study the mechanism and nature of active centers, but surprisingly only few papers about c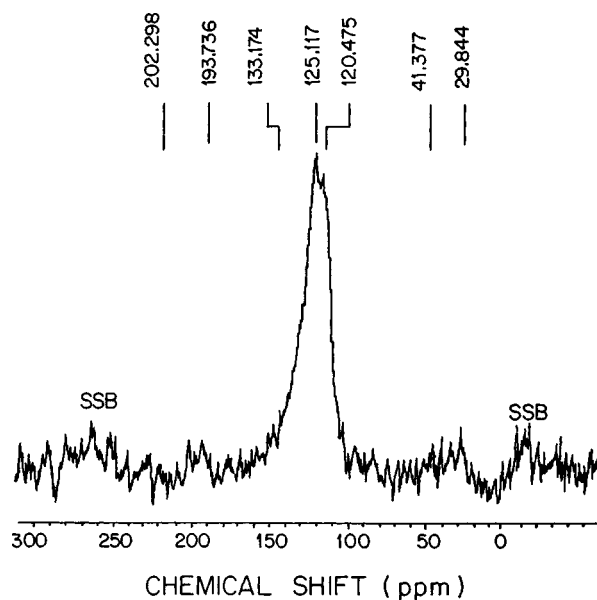oke formation are published, and none concerning with metal supported reforming catalysts [25,26]. In the present work EPR measurements were used to analyze the coke formation in the Pt–Sn/γ-Al$_2$O$_3$ catalyst. Because the EPR signals originating from the free electrons are strongly inhibited when the sample was exposed in air, this indicates that the free electrons are trapped or interacted with the oxygen or water molecules. In order to evaluate such an effect, our EPR measurements were carried out at different temperatures and pressures. The non-coked reforming catalyst did not produce any signal. In the coked catalyst, a single absorption peak was observed (figure 3) from which the resonance magnetic field difference (ΔH), the g factor and paramagnetic centers concentration (RAD/g-cat) at different conditions were calculated (table 1).

ΔH values varied between 3.5 and 4.4 G, and g factors were around 2.0025. These values are close to those of free electrons, indicating that the paramagnetic centers are radicals, and that the coke composition was similar to that of polynuclear aromatic structures. Such condensed structures contribute to a high concentration of non-localized electrons over the aromatic rings of π orbitals. It was observed that pressure in the sample tube considerably affected the paramagnetic centers concentration; it increased two orders of magnitude after evacuating the tube up to 10^{-4} Torr, which is the result of the desorption of the oxygen or water molecules adsorbed on the coke in vacuum condition.

It is known that in the reforming process coke is produced through hydrogenolysis at faces, edges and corners of the metallic particles, and then diffuses over the support surface in the form of carbide until reaching the interface between platinum and support. These carbonaceous materials can progress in acid sites to begin the polymerization reaction that transforms it into pseudographite [27]. The aromatic products on the reforming catalyst could fur-
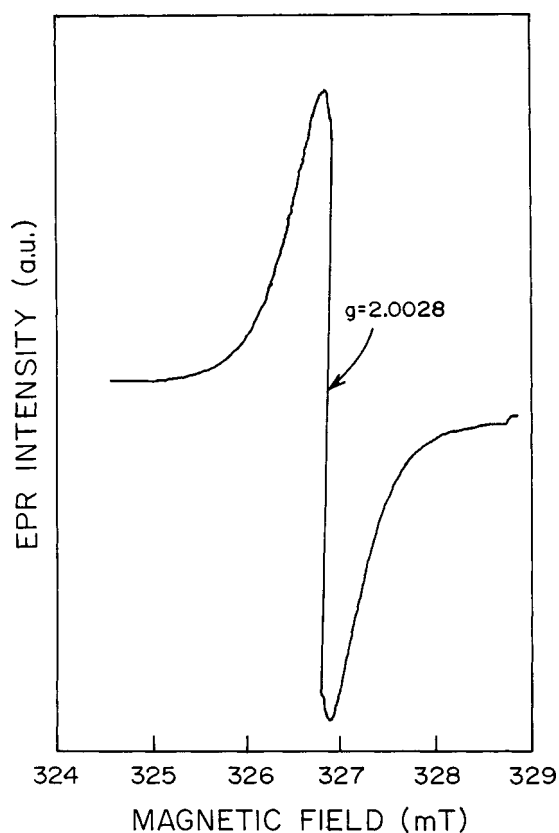
Figure 3. A typical EPR spectrum of the coked Pt–Sn/γ-Al$_2$O$_3$ catalyst.

ther dehydrogenize and polymerize to polynuclear aromatic structures and act as precursors in coke formation.

The X-ray diffraction pattern of the coke separated from the coked catalyst contained only graphite with a larger interlayer structure (0.351 nm) than pure graphite (0.346 nm). The result suggests that this deposited coke might contain unorganized polynuclear aromatic structures with various side groups [15]. In addition, the refinement of the graphite structure by using Rietveld technique showed that coke crystals had an average size of 2.3 nm.

3.2. AFM imaging

AFM imaging has already been proven to be a powerful method for the characterization of surface morphology and other surface properties; for example, phase imaging and micro-elastic mapping [28–31]. AFM has been often used in surface and molecular science, and in electrochemistry and polymer science, and somehow not so often in catalysis, probably because of the complexity of the catalytic material in terms of surface morphology and surface properties.

In many aspects heterogeneous materials are multicomponent and often multifunctional, which are rather difficult to define. Visualization and definition of coke on the catalyst surface is just one of such problems.

In order to characterize the coke from the catalyst substrate surface, in this study we used phase imaging of tapping mode AFM [32–34], a relatively new technique which allows determining surface stiffness and other material mechanical properties, rather that surface morphology. We successfully visualized and recognized the coke film on the catalyst substrate, demonstrating that phase imaging is a valuable tool for such complex visualization process.

Figure 4 shows a typical phase image of the reforming catalyst covered with coke. It seems that the catalyst surface was covered by an amorphous thin film and with disk-like substrate grains that had diameters between 0.3 and 0.5 μm. The coke film appears to be porous with holes between 0.05 and 0.07 μm in diameter [35]. The image shows regions of broken coke film and a catalyst surface free from contamination. Since coke and catalyst differ in their surface characteristics, and therefore, in the way of their interactions with the AFM probe, it is rather easy to distinguish between the surface covered with coke and the free one. Indeed, within the coke film it is possible to see some differences. Namely, beside the continuous coke film some three-dimensional coke clusters of disks with diameters between 0.12 and 0.18 μm were found.

Figure 5 corresponds to the AFM of the regenerated reforming catalyst. In this case, the AFM image reveals two kinds of surface: the catalyst surface which shows large disk-like features that are 0.5 μm in diameter, and small coke clusters ranged in sizes from 0.1 to 0.15 μm. In the image, the substrate appears bright, while coke features are dark and fuzzy. This could indicate that the substrate is harder than the coke agglomerates. Large portions of the coke film are broken. Since the image shows the regenerated reforming catalyst, this indicates that after the regeneration process and possibly during the early stages of coke formation, reaction proceeds via small cluster formation. Clusters were clearly three dimensional, and were distributed randomly all over the surface. Indeed, after tracing in detail the coke position, it was observed that many of the clusters in the image were positioned nearby or directly on the disk-like edges.

3.3. Location and burn-off behavior of deposited coke

The coked catalyst discharged from the industrial reforming process with continuous regeneration had, in av-

Table 1
EPR data obtained under different conditions.

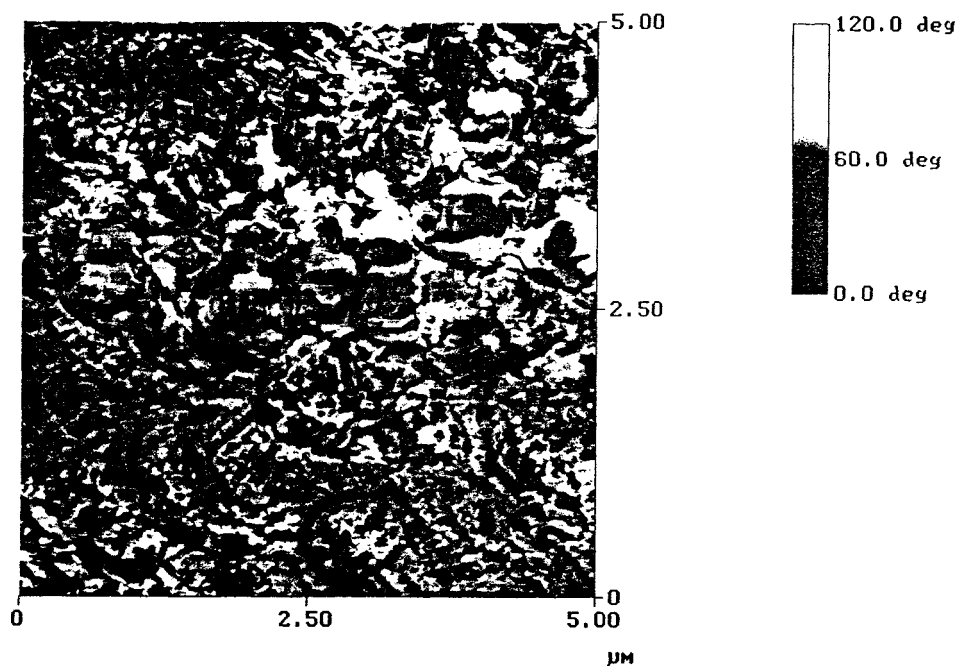|	Room temp.	−160 °C	100 °C (10⁻⁴ Torr)	Room temp. (10⁻⁴ Torr)	−160 °C (10⁻⁴ Torr)
g	2.0025	2.0028	2.0028	2.0028	2.0023
ΔH	4.00	4.8	3.5	4.0	4.0
RAD/g-cat	1.44E+16	1.03E+16	3.84E+18	3.93E+18	4.96E+18

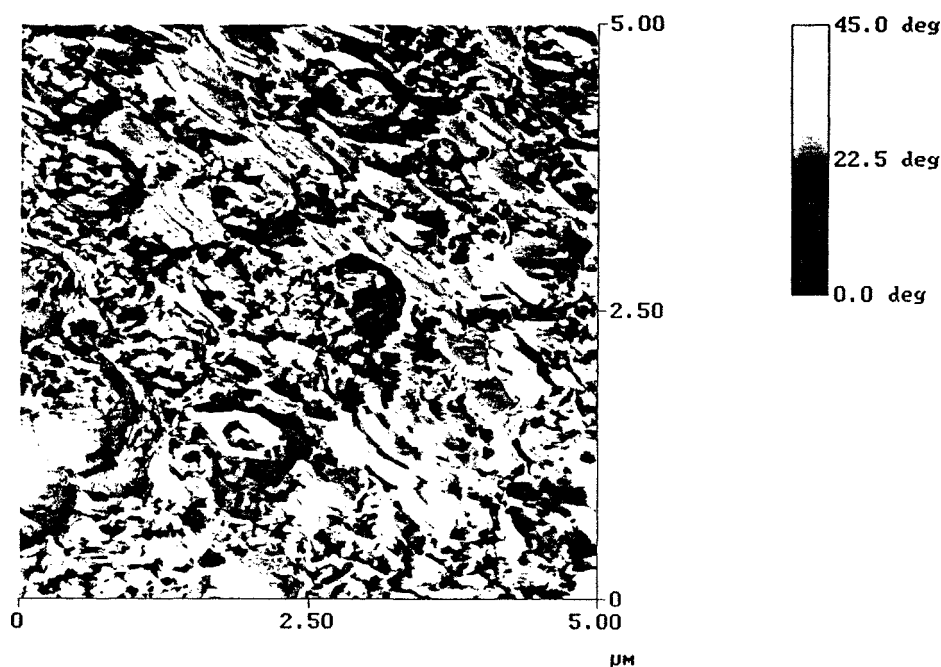Figure 4. Top-view phase image obtained by tapping mode AFM of the coked catalyst.

Figure 5. Top-view phase image obtained by tapping mode AFM of the regenerated catalyst. The coke clusters are darker and rather irregularly shaped, randomly distributed on the catalyst substrate.

erage, a coke content of 4 wt%. For burning the coke off, the catalyst flows from the bottom of the last reactor into the regenerator. The regenerated catalyst, which had only 0.04 wt% coke, was chlorinated to restore its acidity and taken to the top of the first reforming reactor to be reused.

In the present work, adsorption–desorption isotherms were used to characterize the textural modification during the coke formation. As shown in figure 6, the hysteresis loop corresponds to a type II isotherm, which reveals the multilayered mesoporous nature of the catalyst.

The pore size distribution had only one peak at 6.5 nm, ranging between 5.5 and 8.0 nm (figure 7), which is a typical pore distribution of mesoporous solids. These results are in agreement with the Pt–Sn mesoporous catalyst prepared by using the sol–gel method [36]. The most probable capillary diameters remained essentially unchanged during the coke formation. Therefore, we suggest that coke was
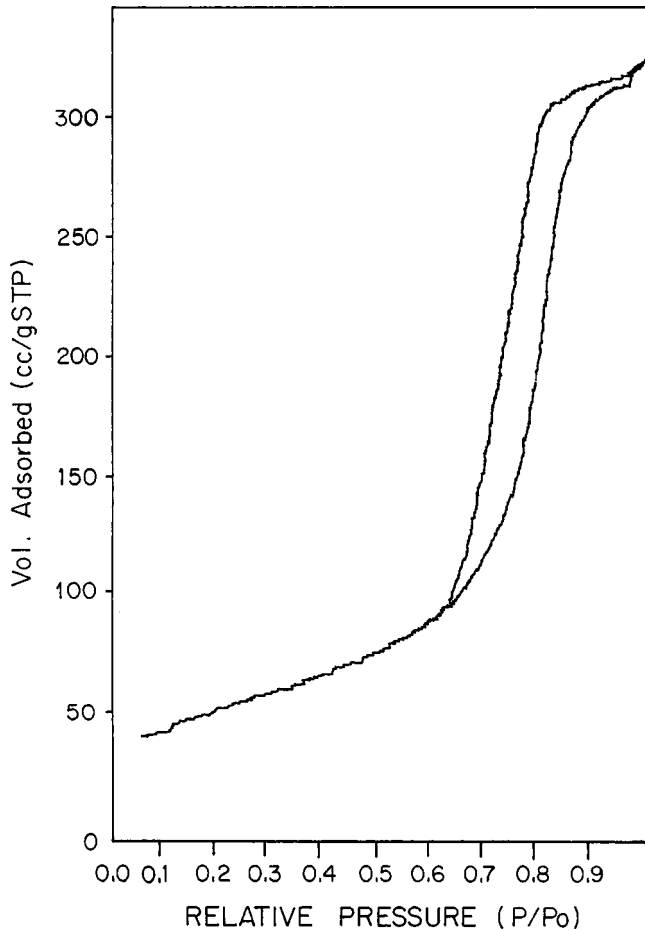
Figure 6. Adsorption–desorption isotherm of the coke Pt–Sn/γ-Al$_2$O$_3$ catalyst.
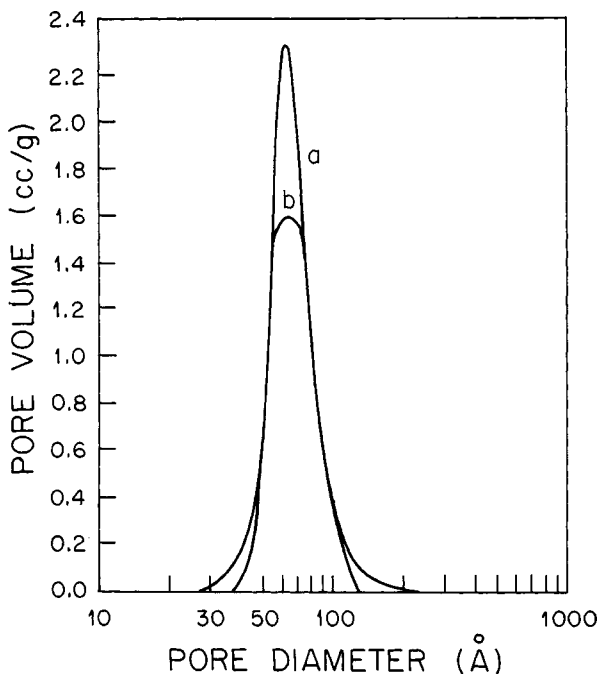
predominantly deposited in the interstitial pores formed between the ultimate particles [37]. Information about the surface areas and the pore volume before and after regeneration are given in table 2.

The DTA and TG-DTG profiles of the coked catalyst are given in figures 8 and 9. The DTA curve had a sharp peak at about 511 °C, which was attributed to the combustion of the coke deposited on the acidic sites of alumina. Meanwhile, a small shoulder-like peak appeared at 245 °C, due to the coke on the metal of the catalyst. These assignments are in good agreement with the other reports [38–40]. The TG curve shows a large weight loss between 339 and 511 °C produced by coke burning off. The above results indicate that the coke was predominantly deposited on the support, and that it can be gasified below 550 °C.

In order to compare with the coke burn-off behavior of the coked catalyst, DTA and TG-DTG profiles of the regenerated catalysts are shown in figures 10 and 11. The DTA curves of these catalysts did not have any peak, which is in accordance with their thermogravimetric analysis. In this case, a first weight loss was observed below 200 °C (figure 11), produced by water desorption; the small peak at 437 °C was caused by the combustion of the residual

Table 2
Specific surface area and pore volume of the fresh and coked catalysts.

Sample	Surface area (m^2/g)	Pore volume (cm^3/g)
Fresh catalyst	203.5	0.5028
Coked catalyst	164.1	0.441

Figure 7. Pore diameter distribution of the coked and regenerated Pt–Sn/γ-Al$_2$O$_3$ catalysts.

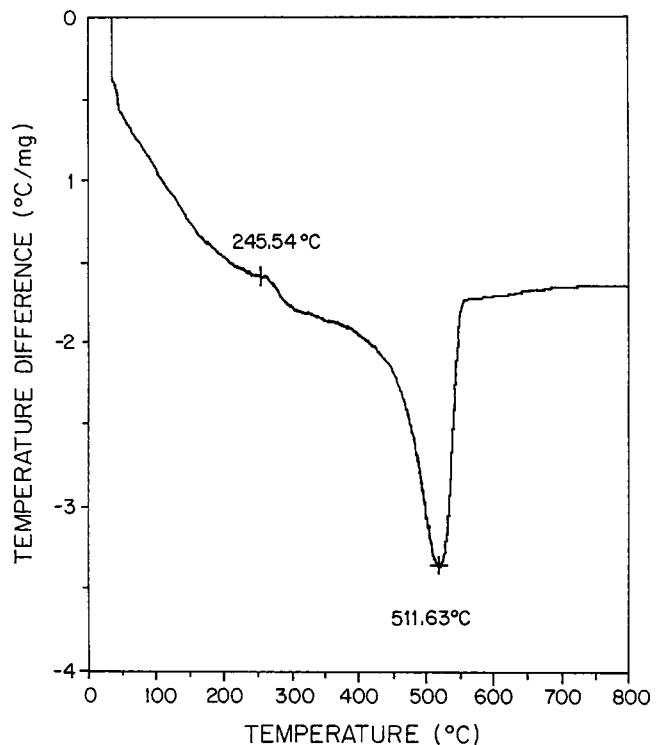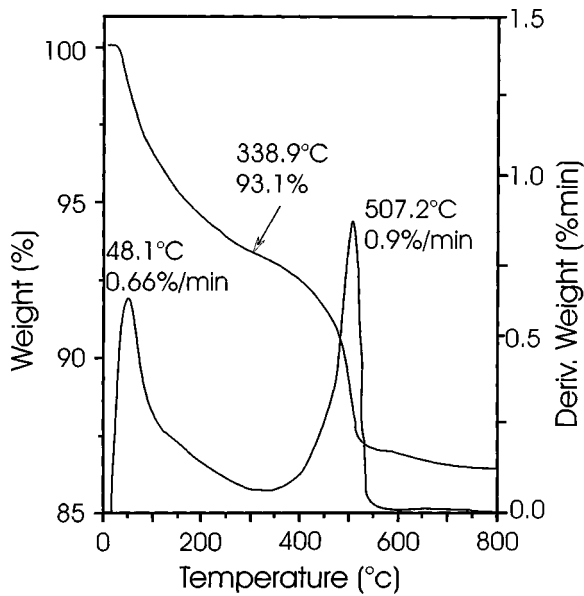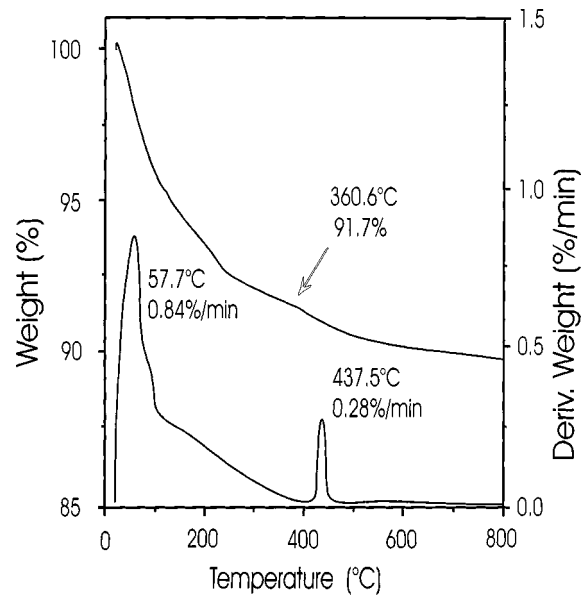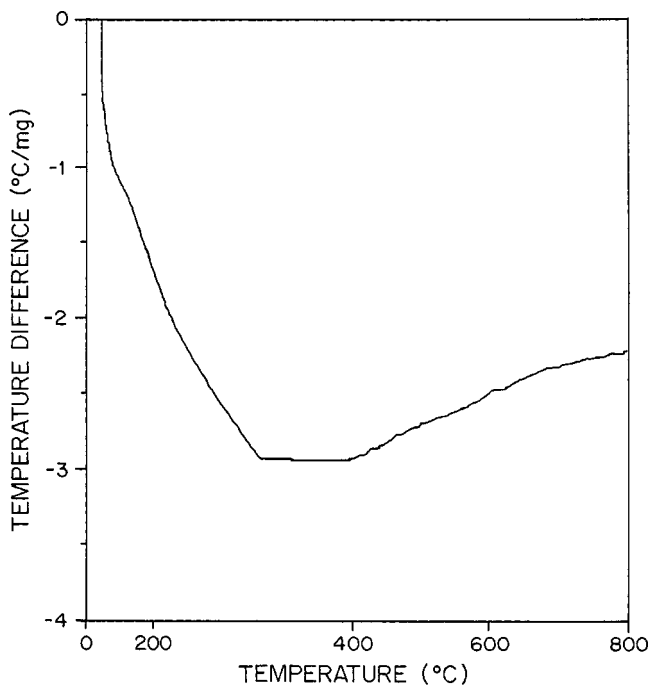Figure 8. DTA curve of the coked Pt–Sn/γ-Al$_2$O$_3$ catalyst.

Figure 9. DTG and TG curves of the coked Pt–Sn/γ-Al₂O₃ catalyst.

Figure 11. DTG-TG profiles of the regenerated Pt–Sn/γ-Al₂O₃ catalyst.

Figure 10. DTA profile of the regenerated Pt–Sn/γ-Al₂O₃ catalyst.

4. Conclusions

The coke content deposited on the Pt–Sn/γ-Al₂O₃ catalyst of a continuous reforming unit was 4.0 wt%. The results suggest that the coke on the active metal centers diffused away rapidly to the acid sites of the alumina support. Coke precursors were aromatic compounds that transformed into polynuclear aromatics and graphite-like structures with a few side chains. Coke was deposited on the catalyst surface, forming continuous amorphous coke films and three-dimensional coke clusters with diameters between 0.12 and 0.18 μm. After catalyst regeneration, the coke remainder on the catalyst was only 0.04 wt%, forming small coke clusters with diameters between 0.1 and 0.15 μm. Coke burn-off temperature, which determines the catalyst regeneration conditions, was below 550 °C. Finally, it is important to note that AFM, ^{13}C NMR and EPR techniques are very effective for characterizing the coke deposited on reforming catalysts.

Acknowledgement

coke. The above results show that after regeneration most of the coke was burned off. The coke content measurements showed that the residual coke after regeneration was less than 1 wt%. Because the burning off of this residual coke requires high temperature, it actually remains in the regenerated catalyst with the reforming catalyst keeping an equilibrium activity level in the reactor.

The good combustion behaviors resulting from the low polymerization degree and the advantageous location of coke deposition would be the two valid reasons to use the Pt–Sn/γ-Al₂O₃ catalyst in reforming units with continuous coke regeneration.

References

[1] A.M. Brownstein, *Trends in Petrochemical Technology* (Petroleum Publishing Co., Tulsa, OK, 1976) p. 17.
[2] R. Burch, J. Catal. 71 (1981) 348.
[3] R. Prestvik, B. Totdal, C.E. Lyman and A. Holman, J. Catal. 176 (1998) 246.
[4] R. Prestik, K. Molyerd, K. Grande and A. Holman, J. Catal. 174 (1998) 119.

[5] F.H. Ribeiro, A.L. Bonivardi, C. Kim and G.A. Somorjai, J. Catal. 150 (1994) 186.

[6] L.J. Mcpherson and M.F. Olive, in: *Modern Petroleum and Technology*, ed. G.D. Hobson, 5th Ed., Part I (1984).

[7] R. Gomez, V. Bertin, P. Bosch and T. Lopez, Catal. Lett. 21 (1993) 309; J. Catal. 142 (1993) 641.

[8] F.B. Passos, D.A.G. Aranda and M. Schmal, J. Catal. 178 (1998) 478.

[9] T. Lopez, M. Asomoza and R. Gomez, Mater. Lett. 19 (1994) 193.

[10] G.T. Baronettic, S.R. Demignel, O.A. Scelza, M.A. Fritzler and A.A. Castro, Appl. Catal. 19 (1985) 77.

[11] K. Balehrishnan and J. Schnank, J. Catal. 127 (1991) 287.

[12] D.L. Trimm, in: *Progress in Catalyst Deactivation*, ed. J.L. Figueiredo (Nijhoff, The Hague, 1982) p. 17.

[13] J. Barbier, in: *Catalyst Deactivation*, eds. B. Delmon and G.F. Froment (Elsevier, Amsterdam, 1987) p. 1.

[14] M. Parera, R.J. Verderone, C.L. Pieck and E.M. Traffand, Appl. Catal. 23 (1986) 15.

[15] N.S. Figoli, J.N. Beltramini, C.A. Querini and J.M. Parera, Appl. Catal. 26 (1986) 39.

[16] J. Barbier, Appl. Catal. 23 (1986) 225.

[17] G.J. Arteaga, J.A. Anderson and C.H. Rochester, Catal. Lett. 58 (1999) 189.

[18] O.A. Barias, A. Holmen and E.A. Blekkan, J. Catal. 158 (1996) 1.

[19] B.H. Li and R.D. Gonzalez, Catal. Lett. 1–2 (1998) 5.

[20] D.A. Best and B.W. Wojciechowski, J. Catal. 47 (1977) 11.

[21] D. Eisenbach and E. Gallei, J. Catal. 56 (1979) 377.

[22] P. Andy, N.S. Gnep, M. Guisnet, E. Benazzi and C. Travers, J. Catal. 173 (1998) 326.

[23] L. Kubelkova, J. Cejka, J. Novakova, V. Bosacek, I. Jirka and P. Jiru, in: *Zeolites, Facts, Figures, Future*, Stud. Surf. Sci. Catal., Vol. 49, eds. P.A. Jacobs and R.A. van Santen (Elsevier, Amsterdam, 1989) p. 1203.

[24] N.G. Kalinina, V.A. Poluboyarov, V.F. Anufrienko and K.G. Ione, Kinet. Catal. 27 (1986) 215.

[25] N.G. Kalinina, Y.V. Ryabov, L.L. Korobitsyna, V.A. Poluboyarov, V.I. Erofeev, L.N. Kurina and V.F. Anufrienko, Kinet. Catal. 27 (1986) 219.

[26] J.T. Ricardson, *Principles of Catalyst Development* (Plenum, New York, 1989) p. 215.

[27] A. Corma, Chem. Rev. 95 (1995) 559.

[28] S.N. Maganov and M.H. Whangbo, in: *Surface Analysis with STM and AFM* (VCH, Weinheim, 1994).

[29] S. Chang, Chem. Rev. 97 (1997) 1017.

[30] C. Rotsch and M. Radmacher, Langmuir 13 (1997) 2825.

[31] E.A. Hassan, W.F. Heinz, M.D. Antonik, N.P. D'Costa, S. Nagaswaran, C.A. Schoenenberger and J.H. Hoh, Biophys. J. 5 (1998) 743.

[32] Q. Zhong, D. Innis, K. Kjoller and V.B. Elings, Surf. Sci. Lett. 290 (1993) L688.

[33] R. Brandsch, G. Bar and M.H. Whangbo, Langmuir 13 (1997) 6349.

[34] G. Bar, R. Brandsch and M.H. Whangbo, Langmuir 14 (1998) 7343.

[35] N. Batina, L.M. Ioffe and Y.G. Borodko, in: *Catalyst Deactivation*, Stud. Surf. Sci. Catal., Vol. 111, eds. C.H. Bartholomew and G.A. Fuentes (Elsevier, Amsterdam, 1997) p. 655.

[36] T. López, M. Asomoza and R. Gómez, Mater. Lett. 19 (1994) 199.

[37] R.G. Haldeman and M.C. Botty, J. Phys. Chem. 63 (1959) 4489.

[38] A. Sárkány, H. Lieske, T. Szilágyi and L. Tóth, in: *8th Int. Congr. Catal.*, Berlin, Vol. 2 (1984) p. 613.

[39] G. Webb, Catal. Today 7 (1990) 139.

[40] C.L. Li, O. Navaro, E. Muñoz, J.L. Boldú, X. Bokhimi, J.A. Wang, T. Lopez and R. Gómez, Appl. Catal., in press.

[41] A.B. Phadnis and V.V. Deshpande, Thermochim. Acta 62 (2983) 361.